MINER'S CUMULATIVE DAMAGE VIA RAINFLOW CYCLE COUNTING
Revision G

By Tom Irvine
Email: tom@vibrationdata.com

July 1, 2014

Vibration fatigue calculations are "ballpark" calculations given uncertainties in S-N curves, stress concentration factors and other variables. Perhaps the best that can be expected is to calculate the accumulated fatigue to the correct "order-of-magnitude."

Introduction

This example is an innovation upon a similar problem in References 1 and 2. It uses a more conservative method than that in Reference 2.

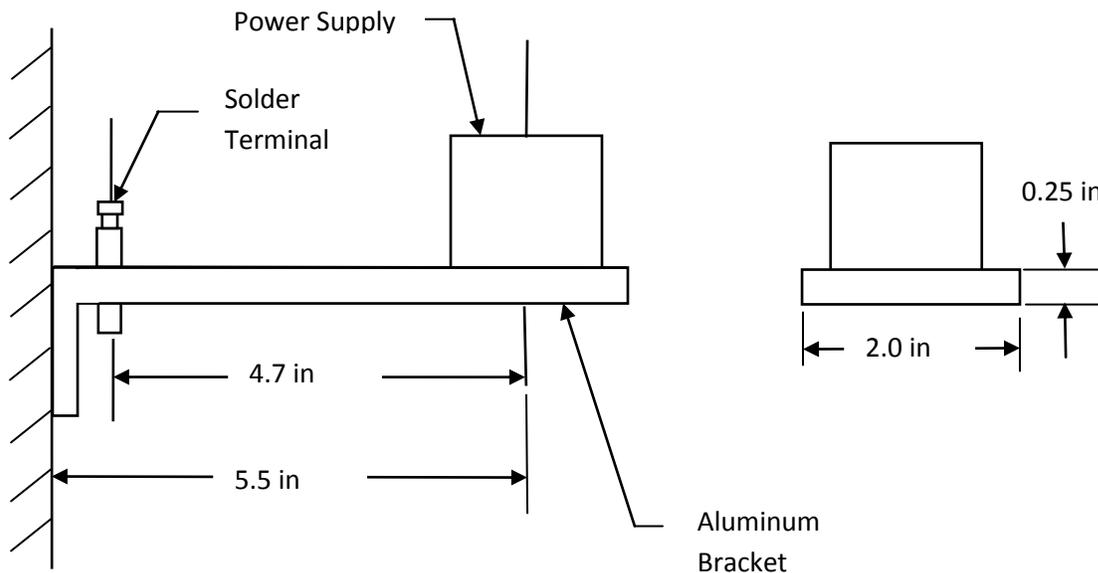Consider a power supply mounted on a bracket as shown in Figure 1.

Figure 1.

The model parameters are

Power Supply Mass	M = 0.44 lbm= 0.00114 lbf sec^2/in
Bracket Material	Aluminum alloy 6061-T6
Mass Density	ρ=0.1 lbm/in^3
Elastic Modulus	E= 1.0e+07 lbf/in^2
Viscous Damping Ratio	0.05

The area moment of inertia of the beam cross-section I is

$$I = \frac{1}{12} b h^3 \tag{1}$$

$$I = \frac{1}{12} [2.0 \text{in}][0.25 \text{in}]^3 \tag{2}$$

$$I = 0.0026 \text{ in}^4 \tag{3}$$

The stiffness EI is

$$EI = [1.0e + 07 \text{ lbf /in^2}][0.0026 \text{ in}^4] \tag{4}$$

$$EI = 2.60e + 04 \text{ lbf in}^2 \tag{5}$$

The mass per length of the beam, excluding the power supply, is

$$\rho = [0.1 \text{ lbm/in}^3][2.0 \text{in}][0.25 \text{in}] \tag{6}$$

$$\rho = 0.05 \text{ lbm/in} \tag{7}$$

The beam mass is

$$\rho L = \left[0.05 \text{ lbm/in\textasciicircum 3}\right]\left[5.5 \text{ in}\right] \tag{8}$$

$$\rho L = 0.275 \text{ lbm} = 0.000712 \text{ lbf sec\textasciicircum 2/in} \tag{9}$$

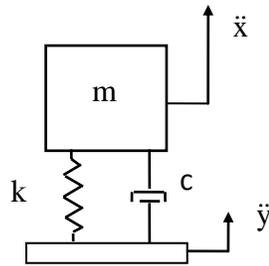Model the system as a single-degree-of-freedom system subjected to base input as shown in Figure 2.

Figure 2.

The natural frequency of the beam, from Reference 3, is given by

$$f_n = \frac{1}{2\pi}\sqrt{\frac{3EI}{(0.2235\,\rho L + m)L^3}} \tag{10}$$

$$f_n = \frac{1}{2\pi}\sqrt{\frac{3\left(2.60e + 04 \text{ lbf in}^2\right)}{(0.2235\,(0.000712 \text{ lbf sec\textasciicircum 2/in}) + (0.00114 \text{ lbf sec\textasciicircum 2/in}))(5.5 \text{ in})^3}} \tag{11}$$

$$f_n = 95.6 \text{ Hz} \tag{12}$$
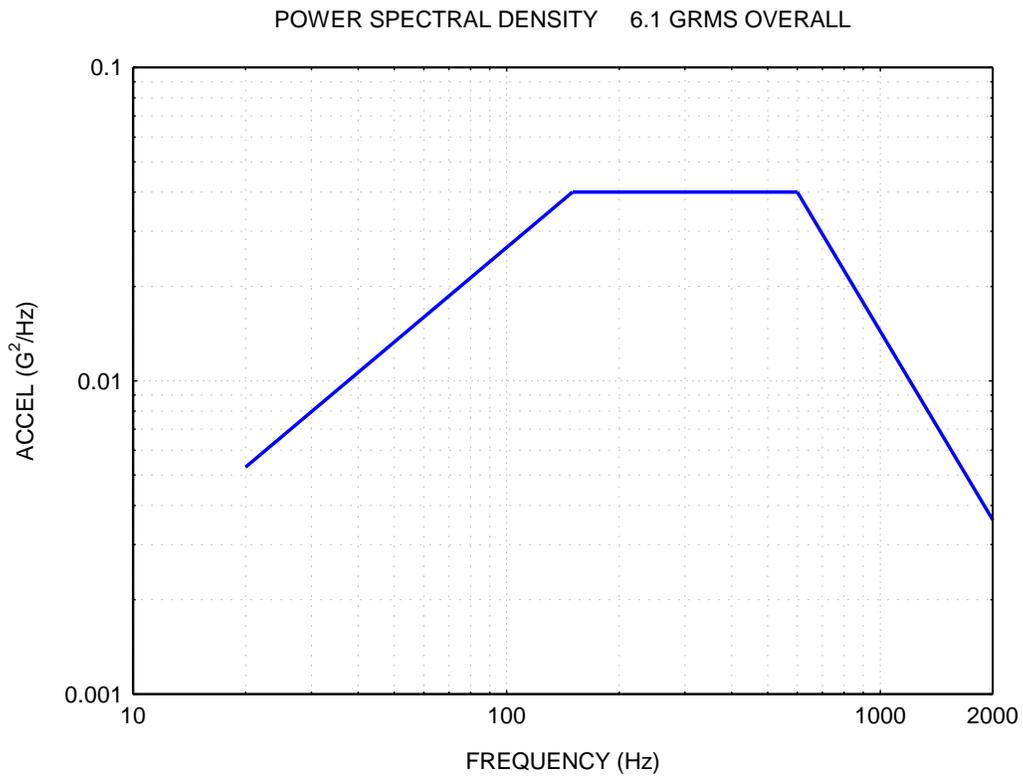
Figure 3.

Table 1. Base Input PSD, 6.1 GRMS	
Frequency (Hz)	Accel (G^2/Hz)
20	0.0053
150	0.04
600	0.04
2000	0.0036

Now consider that the bracket assembly is subjected to the random vibration base input level shown in Figure 3 and in Table 1. The duration is 3 minutes.
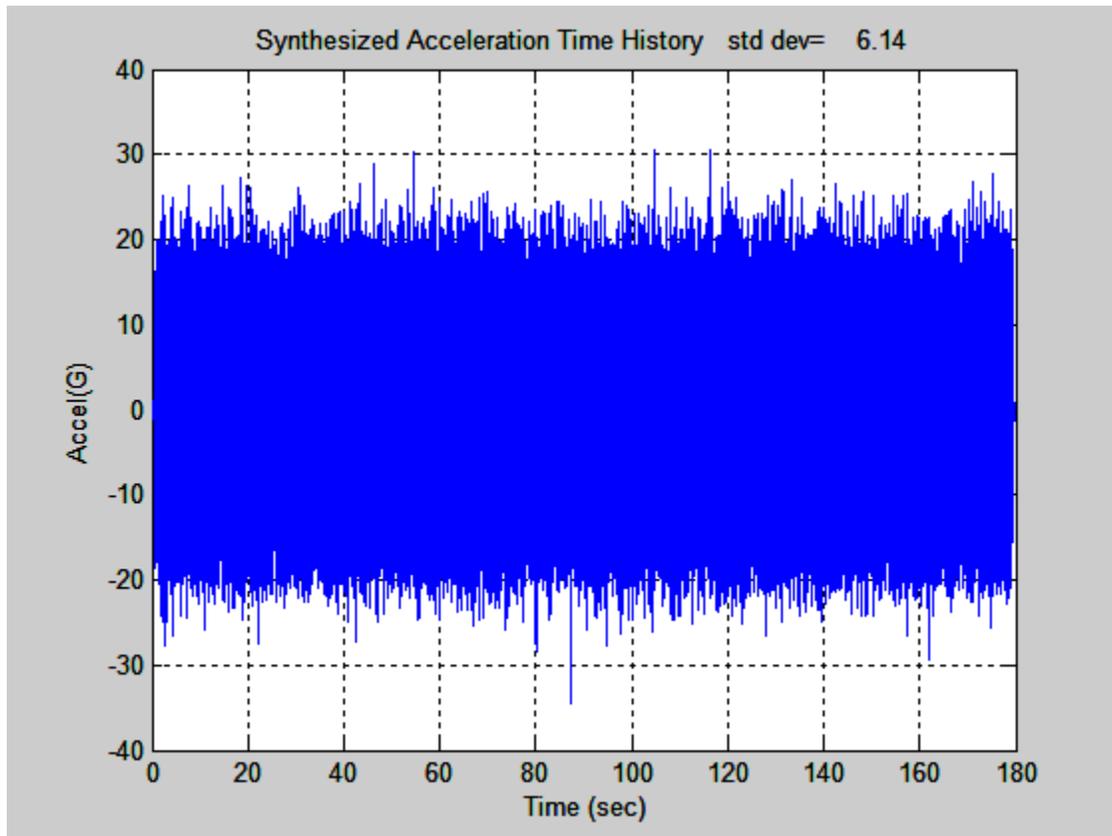
Synthesized Time History

Figure 4.

An acceleration time history is synthesized to satisfy the PSD specification from Figure 3. The resulting time history is shown in Figure 4. The synthesis method is given in Reference 4.

The corresponding histogram has a normal distribution, but the plot is omitted for brevity.

Note that the synthesized time history is not unique. For rigor, the analysis in this paper could be repeated using a number of suitable time histories.
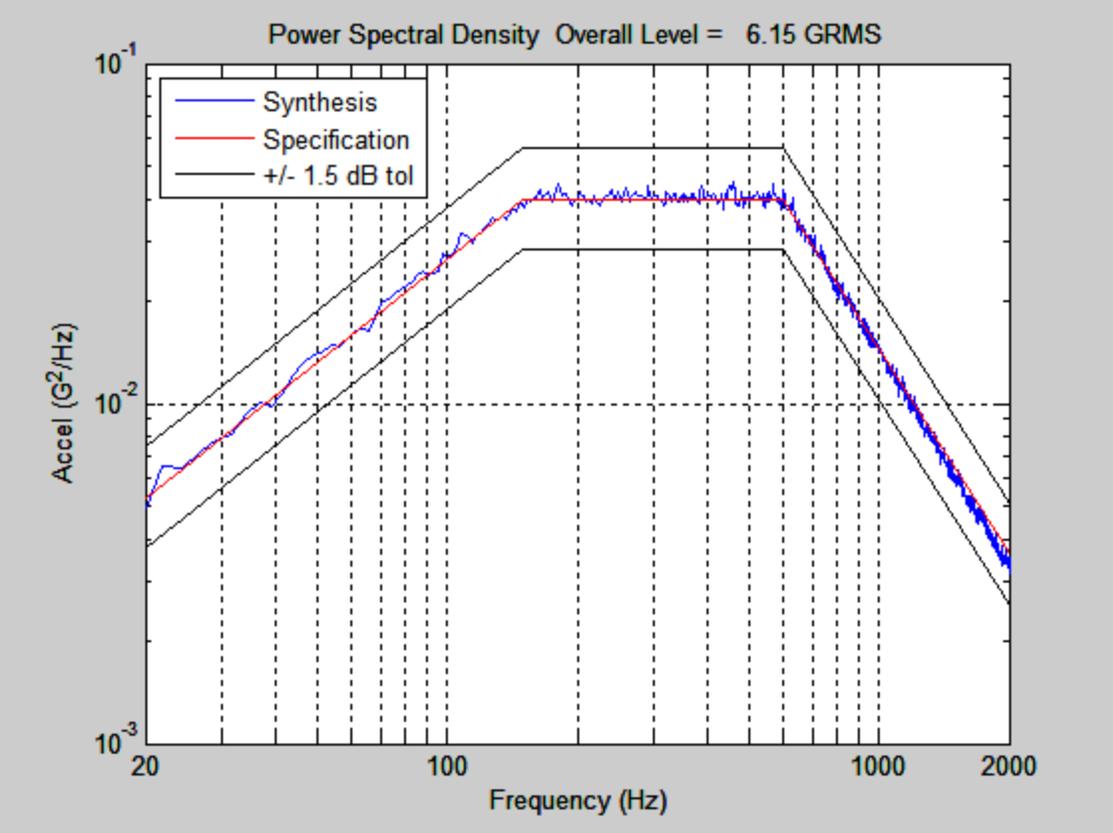
Figure 5.

Verification that the synthesized time history meets the specification is given in Figure 5.
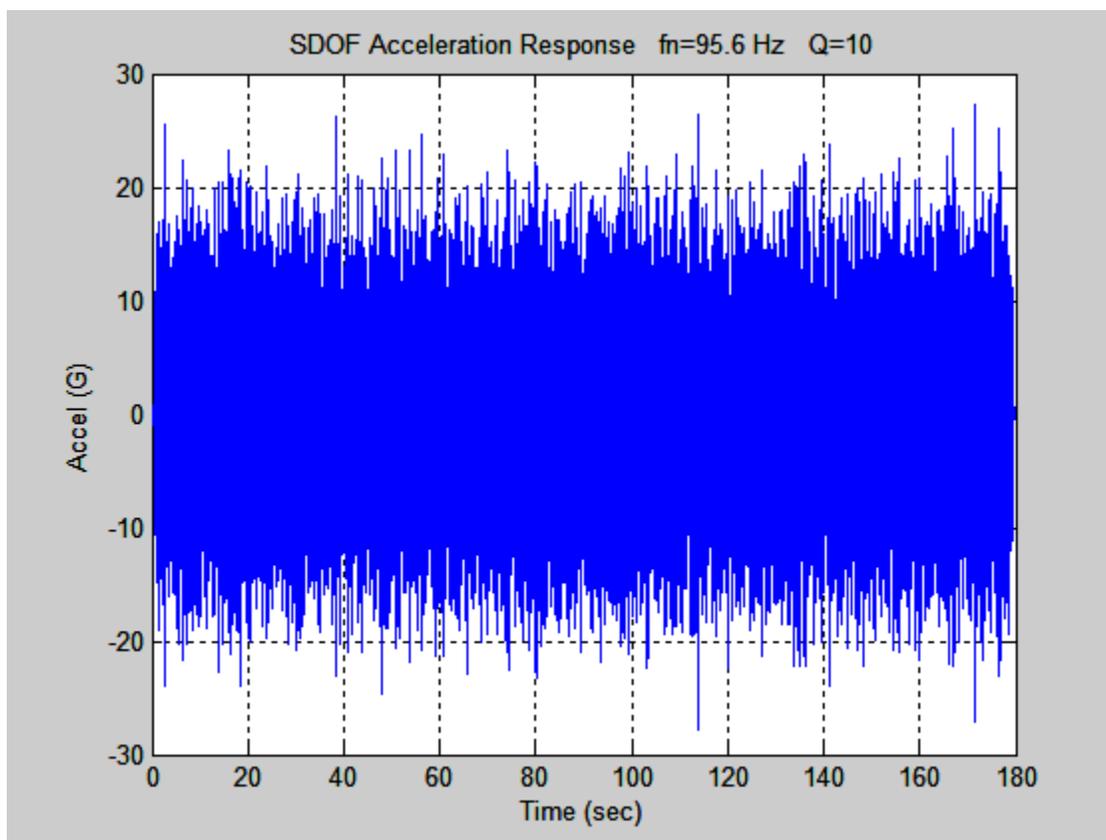
Acceleration Response

Figure 6.

The response acceleration in Figure 6 was calculated via the method in Reference 5. The response is narrowband. The oscillation frequency tends to be near the natural frequency of 95.6 Hz. The histogram has a normal distribution due to the randomly-varying amplitude modulation.

The overall response level is 6.1 GRMS. This is also the standard deviation given that the mean is zero. The response and input levels have the same overall GRMS value, but this only a conicidence.

The absolute peak is 27.8 G, which respresents a 4.52-sigma peak.

Note that some fatigue methods assume that the peak response is 3-sigma and may thus underpredict fatigue damage.

Stress and Moment Calculation
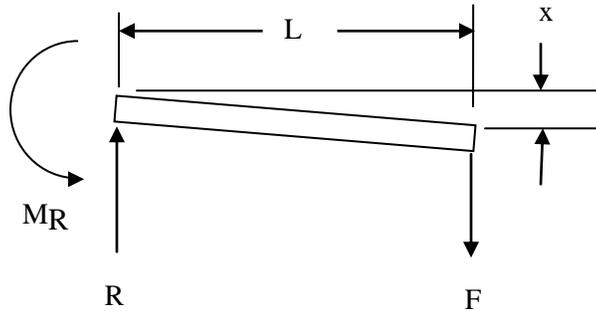
Figure 7.

The following approach is a simplification. A rigorous method would calculate the stress from the strain at the fixed end.

A free-body diagram of the beam is shown in Figure 7.

The reaction moment M_R at the fixed-boundary is

$$M_R = FL \tag{13}$$

The force F is equal to the effect mass of the bracket system multiplied by the acceleration level. The effective mass m_e is

$$m_e = (0.2235 \, \rho L + m) \tag{14}$$

$$m_e = (0.2235 \, (0.000712 \, \text{lbf sec}^2/\text{in}) + (0.00114 \, \text{lbf sec}^2/\text{in})) \tag{15}$$

$$m_e = 0.0013 \, \text{lbf sec}^2/\text{in} \tag{16}$$

The bending moment $\hat{M}$ at a given distance $\hat{L}$ from the force application point is

$$\hat{M} = m_e \, A \hat{L} \tag{17}$$

where A is the acceleration at the force point.

The bending stress S_b is given by

$$S_b = K\hat{M}C/I \tag{18}$$

The variable K is the stress concentration factor. Assume that the stress concentration factor is 3.0 for the solder lug mounting hole.

The variable C is the distance from the neutral axis to the outer fiber of the beam. The cross-section is uniform in the sample problem. Thus C is equal to one-half the thickness, or 0.125 in.

$$S_b(t) = (K m_e \hat{L} C/I)\, A(t) \tag{19}$$

$$(K m_e C/I) = (3.0)(0.0013 \text{ lbf sec\textasciicircum2/in})(5.5 \text{ in})(0.125 \text{ in})/\left(0.0026 \text{ in}^4\right) \tag{20}$$

$$(K m_e C/I) = 1.029 \text{ lbf sec\textasciicircum2/in\textasciicircum3} \tag{21}$$

Apply a unit conversion factor.

$$(K m_e C/I)(386 \text{ (in/sec\textasciicircum2)/G}) = \left(1.029 \text{ lbf sec\textasciicircum2/in\textasciicircum3}\right)(386 \text{ (in/sec\textasciicircum2)/G}) \tag{22}$$

$$(K m_e C/I)(386 \text{ (in/sec\textasciicircum2)/G}) = 397 \text{ (lbf/in\textasciicircum2)/G} \tag{23}$$

$$(K m_e C/I)(386 \text{ (in/sec\textasciicircum2)/G}) = 0.397 \text{ ksi/G} \tag{24}$$
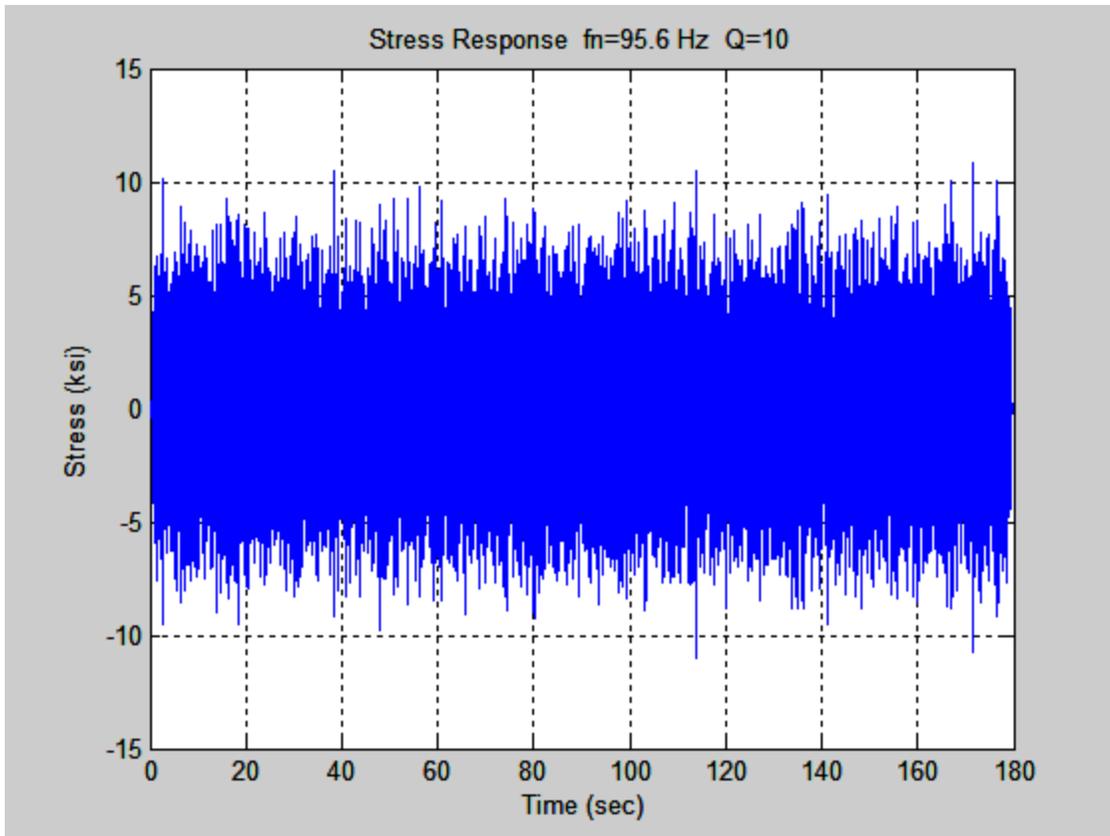
Figure 8.

The standard deviation is 2.4 ksi. The highest absolute peak is 11.0 ksi, which is 4.52-sigma. The 4.52 multiplier is also referred to as the "crest factor."

Next, a rainflow cycle count was performed on the stress time history using the method in Reference 6. The binned results are shown in Table 2.

The binned results are shown mainly for reference, given that this is a common presentation format in the aerospace industry. The binned results could be inserted into a Miner's cumulative fatigue calculation.

The method in this analysis, however, will use the raw rainflow results consisting of cycle-by-cycle amplitude levels, including half-cycles. This brute-force method is more precise than using binned data.

Table 2. Stress Results from Rainflow Cycle Counting, Bin Format, Stress Unit: ksi, Base Input Overall Level = 6.1 GRMS									
Range		Cycle Counts	Average Amplitude	Max Amp	Min Mean	Average Mean	Max Mean	Min Valley	Max Peak
Upper Limit	Lower Limit								
19.66	21.84	3.5	10.43	10.92	-0.29	0.073	0.54	-11.02	10.82
17.47	19.66	21.0	9.11	9.80	-0.35	0.152	0.58	-9.82	10.11
15.29	17.47	108.0	8.07	8.70	-1.36	0.002	0.67	-9.53	9.09
13.10	15.29	372.0	6.98	7.63	-1.07	-0.026	0.71	-8.51	8.34
10.92	13.10	943.0	5.94	6.55	-1.02	0.006	1.00	-7.16	7.20
8.74	10.92	2057.5	4.86	5.46	-1.23	-0.010	0.98	-6.54	6.15
6.55	8.74	3657.0	3.79	4.37	-1.19	-0.002	1.15	-5.30	5.20
4.37	6.55	4809.5	2.72	3.28	-1.02	0.002	1.06	-4.22	4.13
3.28	4.37	2273.5	1.92	2.18	-0.93	0.005	0.94	-3.06	2.94
2.18	3.28	1741.5	1.39	1.64	-0.89	0.002	0.92	-2.36	2.56
1.09	2.18	1140.0	0.83	1.09	-1.04	0.020	1.24	-2.03	1.98
0.55	1.09	670.0	0.40	0.55	-1.63	-0.003	1.86	-1.92	2.40
0.00	0.55	9743.0	0.04	0.27	-6.00	-0.024	5.83	-6.01	5.84

The Range in Table 2 is peak-to-valley.

The Average and Maximum Amplitudes are each equal to (peak-valley)/2

Miner's Cumulative Fatigue

Let n be the number of stress cycles accumulated during the vibration testing at a given level stress level represented by index i.

Let N be the number of cycles to produce a fatigue failure at the stress level limit for the corresponding index.

Miner's cumulative damage index R is given by

$$R = \sum_{i=1}^{m} \frac{n_i}{N_i} \tag{25}$$

where m is the total number of cycles or bins depending on the analysis type.

In theory, the part should fail when

$$Rn \text{ (theory)} = 1.0 \tag{26}$$

For aerospace electronic structures, however, a more conservative limit is used

$$Rn(aero) = 0.7 \tag{27}$$

The number of allowable cycles for a given stress level is determined from an S-N fatigue curve in Appendix A, Figure A-4 for the 6061-T6 aluminum bracket in the sample problem.

Input Level Study

Table 4. SDOF System, Solder Terminal Location, Fatigue Damage Results for Various Input Levels, 180 second Duration, Crest Factor = 4.52			
Input Overall Level (GRMS)	Input Margin (dB)	Response Stress Std Dev (ksi)	R
6.1	0	2.4	7.4e-08
8.7	3	3.4	2.0e-06
12.3	6	4.9	5.3e-05
17.3	9	6.9	0.00142
24.5	12	9.7	0.038
27.4	13	10.89	Ultimate Failure

The accumulated fatigue damage was calculated for a family of cases as shown in Table 4. Each case used the base input PSD from Figure 4 with the indicated added margin. Furthermore, each used a scaled version of the same synthesized time history.

Each full and half-cycle from the rainflow results was accounted for. An allowable N value was calculated for each stress amplitude S using equation (28) for each cycle or half-cycle.

A running summation was made using equation (25).

Again, the success criterion was R < 0.7. The fatigue failure threshold is somewhere between the 12 and 13 dB margin.

The data shows that the fatigue damage is highly sensitive to the base input and resulting stress levels.

Duration Study

A new, 720-second signal was synthesized for the 6 dB margin case.   The time history plot is omitted for brevity.

A fatigue analysis was then performed using the SDOF system in Figure 1. The analysis was then repeated using the 0 to 360 sec and 0 to 180 sec segments of the new synthesized time history. The R values for these three cases are shown in Table 5.

Table 5. SDOF System, Solder Terminal Location, Fatigue Damage Results for Various Durations, 12.2 GRMS Input			
Duration (sec)	Stress RMS (ksi)	Crest Factor	R
180	4.82	4.65	5.37e-05
360	4.89	4.91	0.000123
720	4.89	4.97	0.000234

The R value is approximately directly proportional to the duration, such that a doubling of duration nearly yields a doubling of R.

Time History Synthesis Variation Study

A set of time histories was synthesized to meet the base input PSD + 6 dB. The response of the SDOF system in Figure 1 was calculated. The results are given in Tables 6 and 7.

Table 6. SDOF System, Solder Terminal Location, Fatigue Damage Results for Various Time History Cases, 180-second Duration, 12.2 GRMS Input			
Stress RMS (ksi)	Crest Factor	Kurtosis	R
4.86	5.44	3.1	6.99E-05
4.89	4.40	3.0	5.18E-05
4.80	4.43	3.0	4.93E-05
4.90	4.46	3.1	7.06E-05
4.89	5.79	3.0	7.60E-05
4.88	4.95	3.0	6.02E-05
4.84	4.64	3.0	4.76E-05
4.82	4.65	3.1	5.37E-05
4.81	4.37	3.0	4.38E-05
4.86	4.57	3.0	5.30E-05
4.84	4.60	3.0	5.11E-05
4.86	4.27	3.0	4.67E-05

Table 7. Limits for Stress Response Parameters		
Parameter	Min	Max
Stress (ksi)	4.80	4.90
Crest Factor	4.27	5.79
Kurtosis	2.99	3.12
R	4.38E-05	7.60E-05

Note that the crest factor is the ratio of the peak-to-standard deviation, or peak-to-rms assuming zero mean.

Note that Rayleigh distribution predicts a 4.55 crest factor for a 95.6 Hz oscillator over a 180-second duration. The formula is given in Appendix B.

The crest value varies such that the maximum value is 36% higher than the minimum.

The overall stress level and kurtosis remain nearly constant across the set of time histories. Kurtosis is defined in Appendix C.

The R value varies with the maximum being 73% higher than the minimum.

The R value is sensitive to the overall stress RMS level, crest factor and kurtosis, tending to increase with even small positive changes in each of these parameters. See Figures 9 through 11, which include a linear curve-fit.
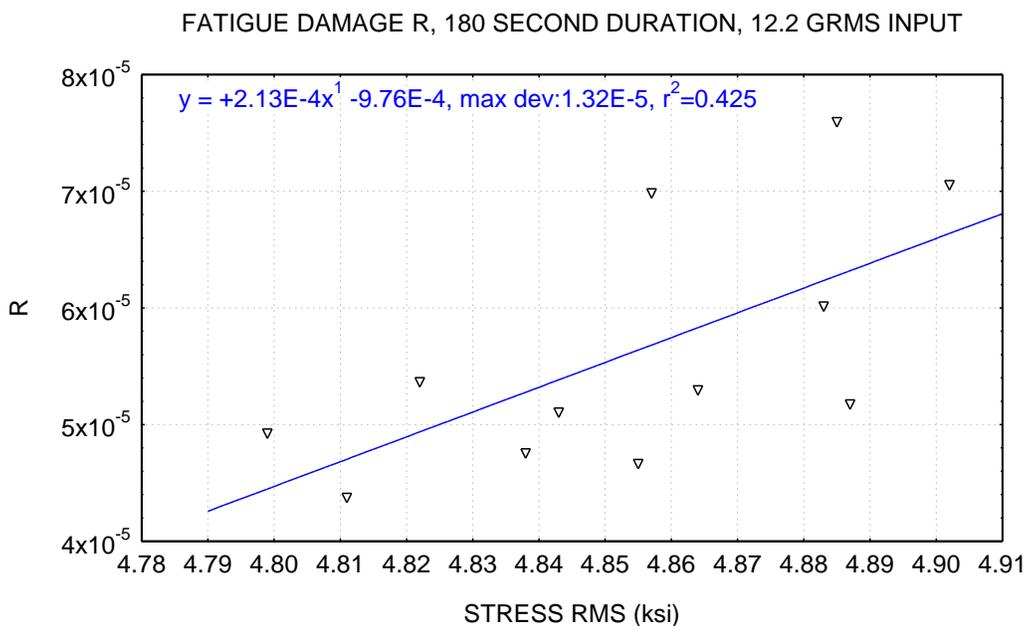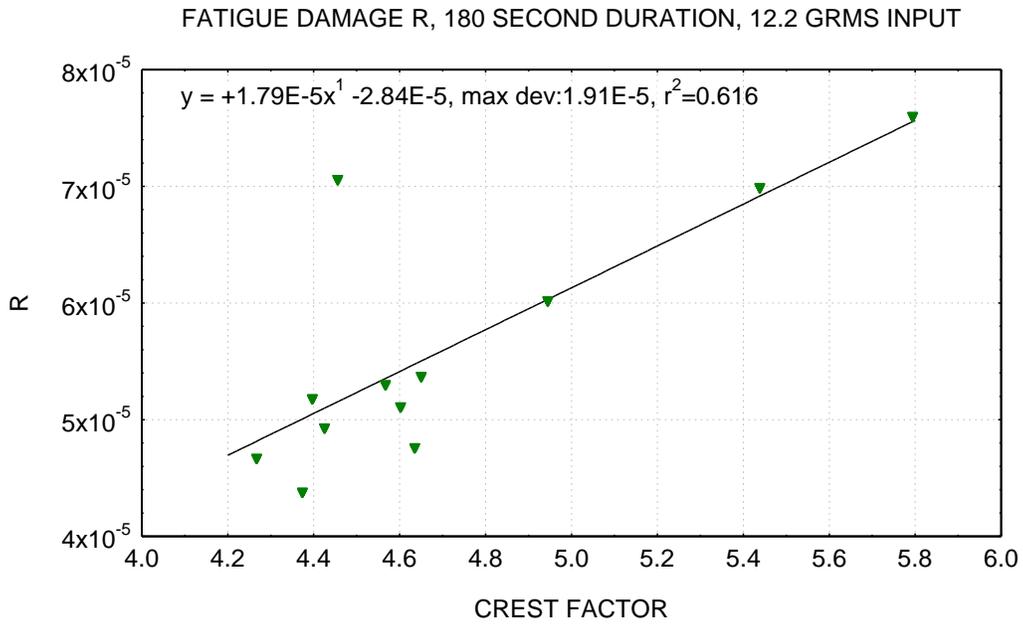
FATIGUE DAMAGE R, 180 SECOND DURATION, 12.2 GRMS INPUT

$$y = +2.13E\text{-}4x^{1} -9.76E\text{-}4, \text{ max dev:}1.32E\text{-}5, r^{2}=0.425$$

Figure 9.

FATIGUE DAMAGE R, 180 SECOND DURATION, 12.2 GRMS INPUT

$y = +1.79E\text{-}5x^1 -2.84E\text{-}5$, max dev:1.91E-5, $r^2 = 0.616$

Figure 10.

FATIGUE DAMAGE R, 180 SECOND DURATION, 12.2 GRMS INPUT

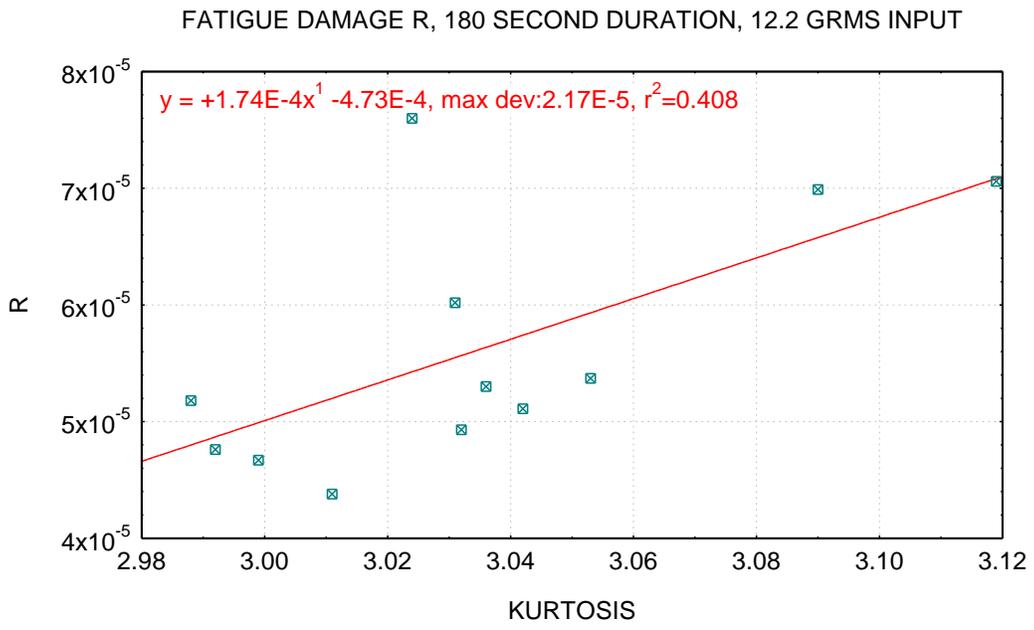$y = +1.74E\text{-}4x^1 -4.73E\text{-}4$, max dev:2.17E-5, $r^2 = 0.408$

Figure 11.

The data in Figures 9 through 11 are a snapshot for a particular SDOF system and base input PSD.

This "Time History Variation" study should be repeated with varying natural frequencies, damping ratios, input levels, durations, etc.

Conclusion

This is a "work-in-progress."

Fatigue analysis already carries uncertainty given that S-N curves and stress concentration factors are both tenuous.

The crest factor and kurtosis are very important. Response peaks above 3-sigma make a significant contribution to fatigue damage. Even minor changes in the response stress can have significant effect on the fatigue damage R.

The results in Figure 6 show variation in the fatigue damage R with a set of independent base input time histories each of which satisfies the same base input PSD specification. The difference is due variation in underlying response statistical parameters. A conservative approach for a given design problem would thus be to take the maximum R for ten or more independent synthesis cases.

Note that the stress response variation would also occur for a shaker table test, even if the base input is peak-limited.

There are addition concerns arising from modeling simplifications.

The analysis used pure bending stress. A better approach would have been to use the maximum principal stress or von Mises stress which would have included the shear stress. The stress contributions of higher modes should also be considered.

There are additional material concerns as given in Appendix D.

Idealizing a system as a single-degree-of-freedom system may yield to an under-prediction of the fatigue damage as shown in Appendix E. The inclusion of higher modes may not increase the stress level much but will increase the fatigue damage, because higher modes add relatively high-frequency stress reversal cycles.

Additional Applications

The fatigue method is applied to a continuous beam model in Appendix E.

References

1. Dave Steinberg, Vibration Analysis for Electronic Equipment, Second Edition, Wiley, New York, 1988.

2. T. Irvine, Random Vibration Fatigue, Revision B, Vibrationdata, 2003.

3. T. Irvine, Bending Frequencies of Beams, Rods, and Pipes, Revision S, Vibrationdata, 2012.

4. T. Irvine, A Method for Power Spectral Density Synthesis, Rev B, Vibrationdata, 2000.

5. David O. Smallwood, An Improved Recursive Formula for Calculating Shock Response Spectra, Shock and Vibration Bulletin, No. 51, May 1981.

6. ASTM E 1049-85 (2005) Rainflow Counting Method, 1987.

7. http://en.wikipedia.org/wiki/Fatigue_(material)

8. MIL-HDDK-5J, Department of Defense Handbook: Metallic Materials and Elements for Aerospace Vehicle Structures, 31 Jan 2003.

9. Kathleen S. Dragolich, Nikki D. DiMatteo, Fatigue Data Book: Light Structural Alloys, ASM International.

10. http://scholar.lib.vt.edu/theses/available/etd-07192001-124624/unrestricted/ComeauChapter3doc.pdf

11. K. Ahlin, Comparison of Test Specifications and Measured Field Data, Sound & Vibration, September 2006.

12. V. Adams and A. Askenazi, Building Better Products with Finite Element Analysis, OnWord Press, Santa Fe, N.M., 1999.

13. T. Irvine, Modal Transient Vibration Response of a Cantilever Beam Subjected to Base Excitation, Vibrationdata, 2013.

APPENDIX A

Fatigue S-N Curves

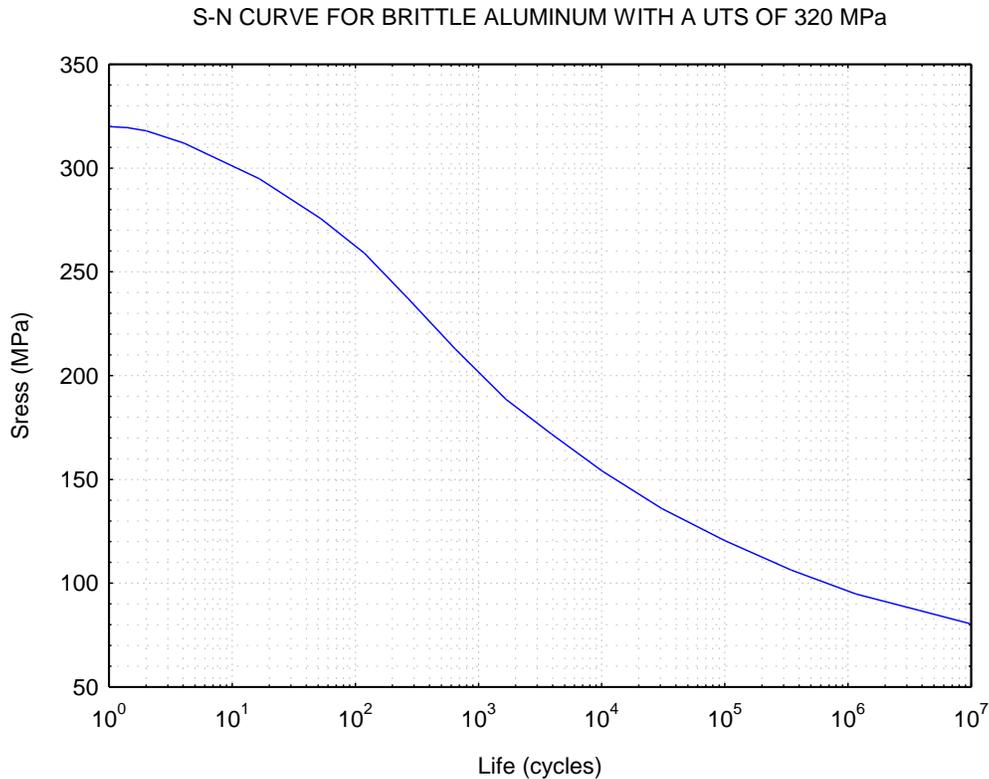S-N CURVE FOR BRITTLE ALUMINUM WITH A UTS OF 320 MPa

Figure A-1.

The curve in Figure A-1 is taken from Reference 7.

It may be unsuitable for engineering calculation because the alloy and other details are unidentified. But it is very useful as a qualitative example of aluminum fatigue.

The curve can be roughly divided into two segments. The first is the low-cycle fatigue portion from 1 to 1000 cycles. This curve is concave as viewed from the origin. The second portion is the high-cycle curve beginning at 1000, which is convex as view from the origin.

Furthermore, the stress level for one cycle is the ultimate stress limit.
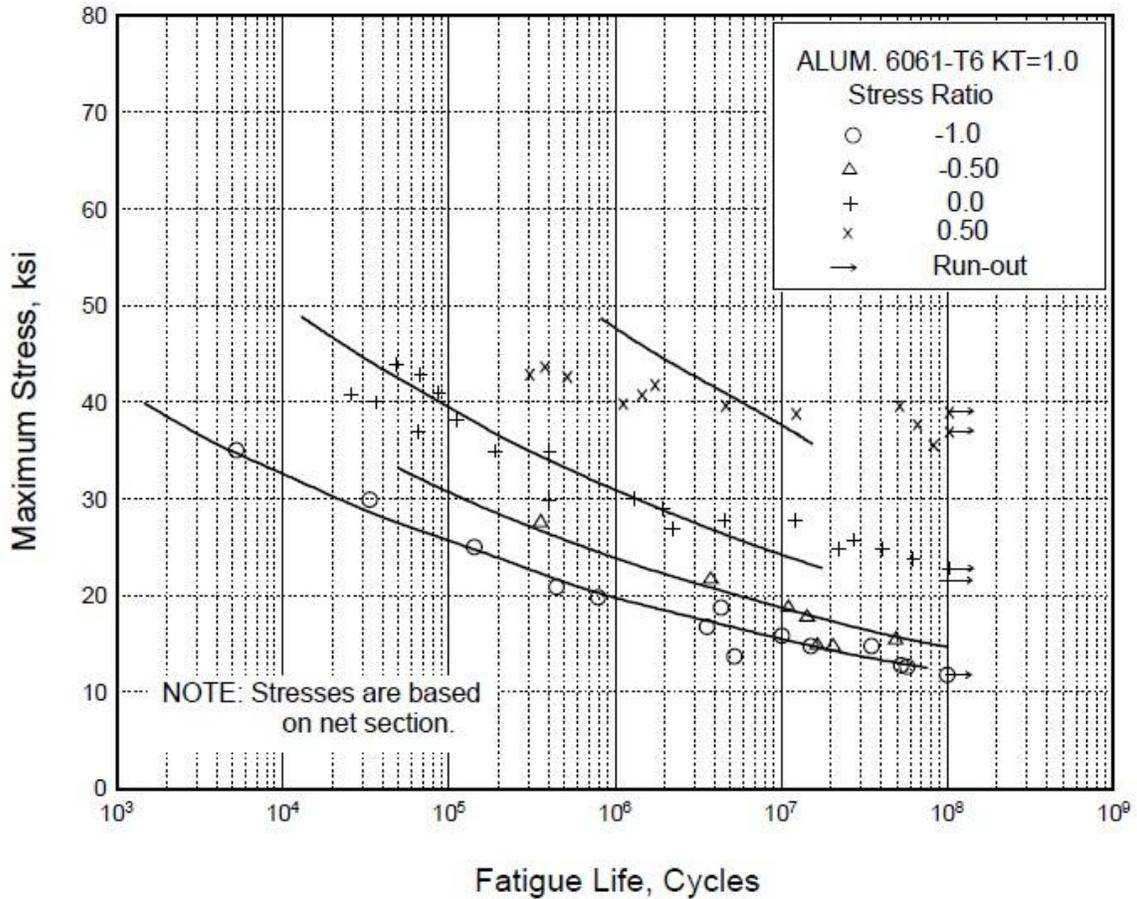
There is no endurance limit.

Figure A-2.

The fatigue curve for aluminum 6061-T6 is shown in Figure A-2, from Reference 8, Figure 3.6.2.2.8.

The stress ratio in the legend is the (peak/valley) for a given cycle. The KT value indicates the stress concentration factor of 1.0.

The ultimate stress for Al 6061-T6 is 45 ksi per Reference 8. The yield stress is 40 ksi.

These stress limits are for the tested samples in Figure A-2. The actual values also depend on the form. Sheet, plate, bars, rods, extrusions, forgings and castings all have their own set of limits.

The advantage of the curve in Figure A-2 is that it is authoritative and well-documented. The disadvantage is that is does not cover low-cycle fatigue below 1000 cycles.
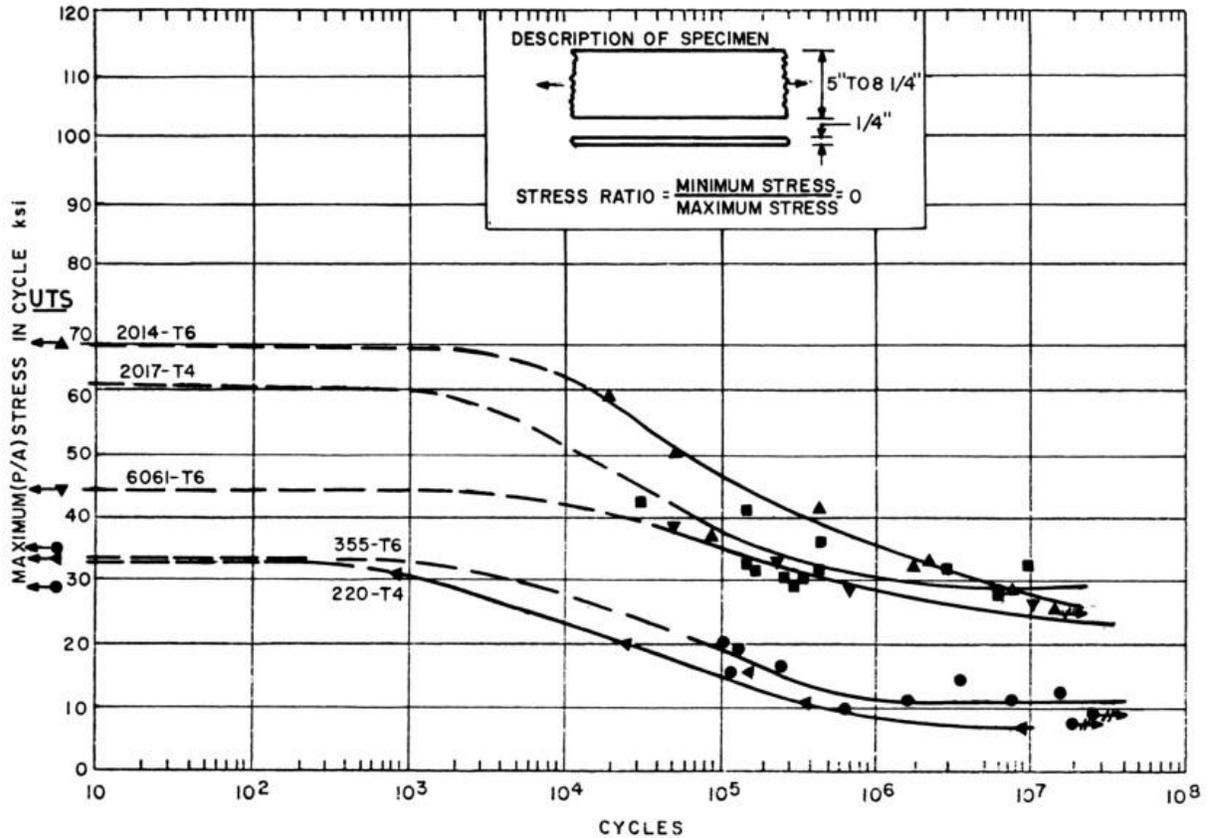
Figure A-3.

The data in Figure A-3 is taken from Reference 9.

The test data for aluminum 6061-T6 appears to begin at $2(10^4)$ cycles. A plateau at the ultimate stress limit of 45 ksi is assumed from 10 to (10^4) cycles.

The plateau has a physical explanation. Hysteresis loops form in the stress-strain curves for materials undergoing cyclical loading where the maximum stress extends into the plastic deformation regime. In particular, aluminum undergoes strain-hardening. Its hysteresis loops stabilize after repeated cycling so that the stress amplitude remains relatively constant over a large portion of fatigue life. Further information is given in Reference 10.

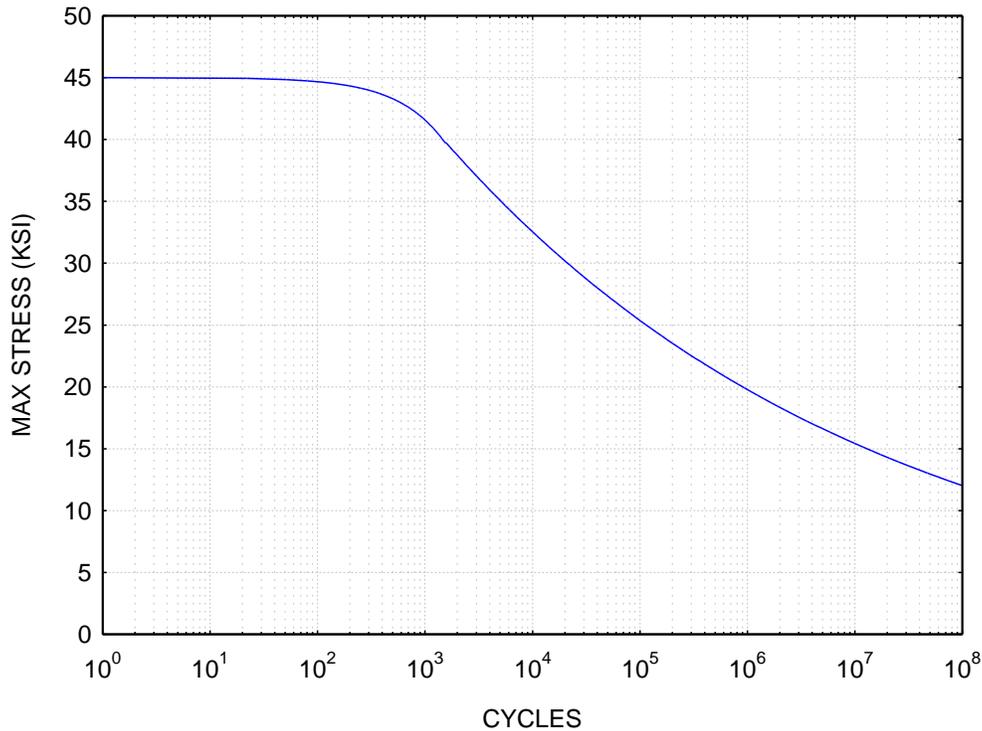S-N CURVE ALUMINUM 6061-T6 KT=1 STRESS RATIO= -1
FOR REFERENCE ONLY

Figure A-4.

The maximum stress is zero-to-peak for the stress ratio = -1.

The purpose of this section is not to give the definitive S-N curve for aluminum 6061-T6, but is rather to give a working curve for the examples in this paper.

The -1 curve will be used for the examples. Note that the -1 ratio roughly meets the expected rainflow cycle behavior.

An extrapolation is made for the low-cycle fatigue region from point (1 cycle, 45 ksi) to (15384 cycles, 39.73 ksi) using a simple linear curve. This is a documented assumption. A thorough consideration of low-cycle fatigue is beyond the scope of this paper.

The curve-fit equations are given as follows.

Let N be the number of cycles. Let S be the corresponding maximum stress amplitude.

The following equation pair applies to the case where N<1538 and S > 39.73 ksi.

$$S = -0.00343 N + 45 \qquad\qquad (A\text{-}1)$$

$$N = -291.727 S + 13128.7 \qquad\qquad (A\text{-}2)$$

Note that the indicated significant digits are required in equation (A-2) for numerical accuracy.

The following equation pair applies to the case where N≥1538 and S ≤ 39.7 ksi.

$$\log_{10}(S) = -0.108 \log_{10}(N) + 1.95 \qquad\qquad (A\text{-}3)$$

$$\log_{10}(N) = -9.25 \log_{10}(S) + 17.99 \qquad\qquad (A\text{-}4)$$

APPENDIX B

Rayleigh Distribution Crest Factor for an SDOF System Response

The formula is for the maximum predicated crest factor C is

$$C = \sqrt{2\ln(\mathrm{fn}\,T)} + \frac{0.5772}{\sqrt{2\ln(\mathrm{fn}\,T)}}$$
(B-1)

   where

         fn   is the natural frequency

         T   is the duration

         ln   is the natural logarithm function

Equation (B-1) is taken from Reference 11.

APPENDIX C

Kurtosis

Kurtosis is a parameter that describes the shape of a random variable's histogram or its equivalent probability density function (PDF).

The kurtosis for a time series Y_i is

$$\text{Kurtosis} = \frac{\sum_{i=1}^{n}[Y_i - \mu]^4}{n\sigma^4}$$

(C-1)

where

μ = Mean

σ = standard deviation

n = number of samples

The term in the numerator is the "fourth moment about the mean."

A pure sine time history has a kurtosis of 1.5.

A time history with a normal distribution has a kurtosis of 3.

Some alternate definitions of kurtosis subtract a value of 3 so that a normal distribution will have a kurtosis of zero.

A kurtosis larger than 3 indicates that the distribution is more peaked and has heavier tails than a normal distribution with the same standard deviation.

Fatigue Cracks

A ductile material subjected to fatigue loading experiences basic structural changes. The changes occur in the following order:

1. *Crack Initiation.* A crack begins to form within the material.

2. *Localized crack growth*. Local extrusions and intrusions occur at the surface of the part because plastic deformations are not completely reversible.

3. *Crack growth on planes of high tensile stress.* The crack propagates across the section at those points of greatest tensile stress.

4. *Ultimate ductile failure.* The sample ruptures by ductile failure when the crack reduces the effective cross section to a size that cannot sustain the applied loads.

Design and Environmental Variables affecting Fatigue Life

The following factors decrease fatigue life.

1. *Stress concentrators.* Holes, notches, fillets, steps, grooves, and other irregular features will cause highly localized regions of concentrated stress, and thus reduce fatigue life.

2. *Surface roughness.* Smooth surfaces are more crack resistant because roughness creates stress concentrators.

3. *Surface conditioning.* Hardening processes tend to increase fatigue strength, while plating and corrosion protection tend to diminish fatigue strength.

4. *Environment.* A corrosive environment greatly reduces fatigue strength. A combination of corrosion and cyclical stresses is called *corrosion fatigue.*

Temperature may also be a factor.

APPENDIX E

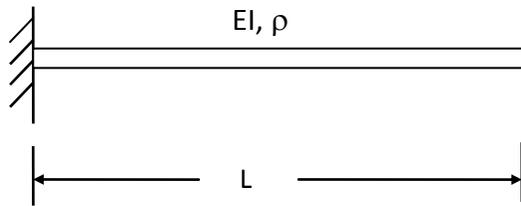Continuous Beam Subjected to Base Excitation

Figure E-1.

The response of a continuous beam to an arbitrary base input can be calculated via Reference 13. This allows the bending stress to be calculated from the strain.

Consider the beam in Figure E-1 with the following properties:

Cross-Section	Rectangular
Boundary Conditions	Fixed-Free
Material	Aluminum

Width	w	=	2.0 in
Thickness	t	=	0.25 in
Length	L	=	12 in
Elastic Modulus	E	=	1.0e+07 lbf/in^2
Area Moment of Inertia	I	=	0.0026 in^4
Mass per Volume	ρ_V	=	0.1 lbm/in^3
Mass per Length	ρ	=	0.05 lbm/in
Viscous Damping Ratio	ξ	=	0.05 for all modes

Calculate the bending stress at the fixed boundary. Omit the stress concentration factor. The base input time history is the same as that in Figure 4 with 21 dB margin.
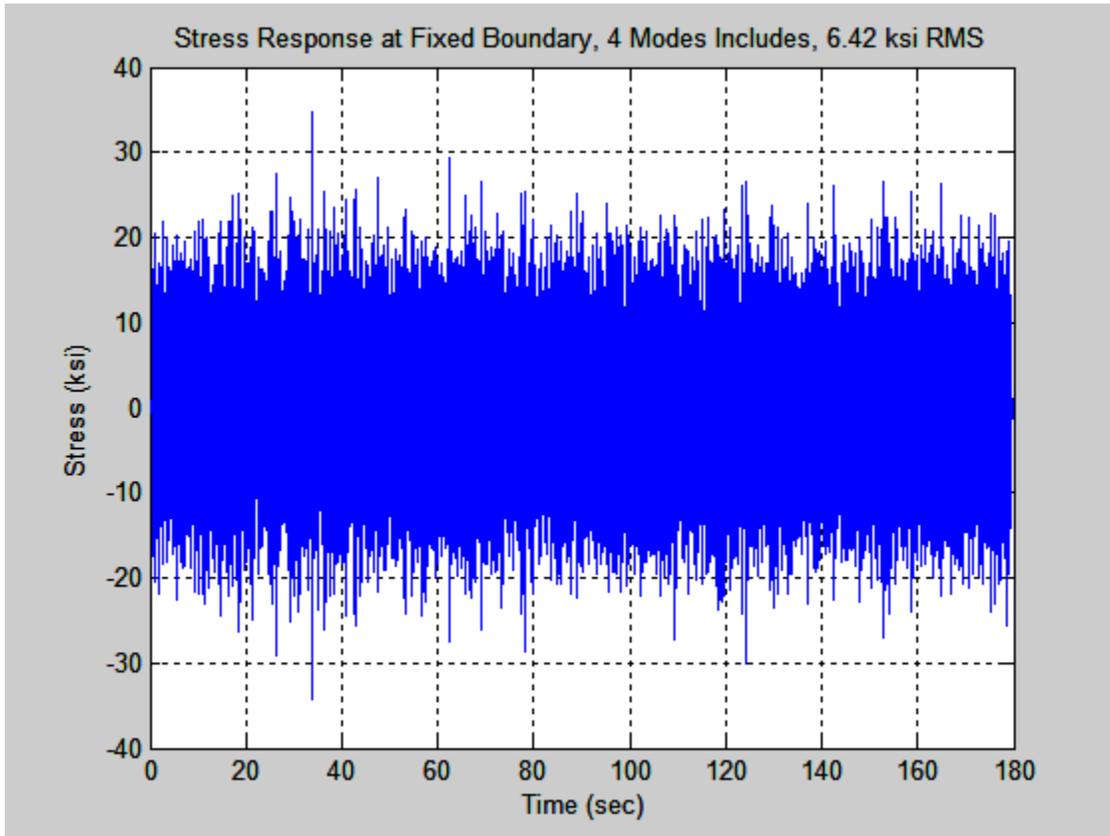

Figure E-2.

The response analysis is performed using Matlab script: continuous_beam_base_accel.m. The normal modes results are given in Table E-1. A typical response is shown in Figure E-2.

Table E-1. Natural Frequency Results, Fixed-Free Beam			
Mode	fn (Hz)	Participation Factor	Effective Modal Mass (lbm)
1	55	0.031	0.368
2	345	0.017	0.113

3	967	0.010	0.039
4	1895	0.007	0.020
5	3132	0.006	0.012

Again, both the mode shape and participation factor are considered as dimensionless, but they must be consistent with respect to one another.

Table E-2. Continuous Beam, Stress at Fixed Boundary, Fatigue Damage Results, 180-second Duration, 68.9 GRMS Input				
Modes Included	Stress RMS (ksi)	Crest Factor	Kurtosis	R
1	6.07	5.78	3.09	0.0004426
2	6.41	5.33	3.08	0.001138
3	6.42	5.37	3.08	0.001243
4	6.42	5.40	3.08	0.001260

The fatigue damage results in Table E-2 would have been higher if a stress concentration factor was included. The purpose of this investigation was rather to determine the effect of including higher modes for a sample continuous system.

The results show that the stress RMS can be accurately calculated using only two modes.

The fatigue damage R reaches at plateau at three modes.

Note that fifth modal frequency is well above the maximum frequency of the base input, so it was neglected.

A more thorough investigation would involve repeating this analysis for a family of time history inputs, either with the same or varying overall levels.

APPENDIX F

Time Scaling for Equivalent Testing

The following applies to structures consisting only of aluminum 6061-T6 material.

It is based on the segment of the S-N curve in Figure A-4 for stress levels below 39.73 ksi.

Rewrite equation (A-3) as

$$\log 10\ (S) \ \propto \ -0.108 \log 10\ (N) \tag{F-1}$$

$$\log 10\ (S) \ \propto \ \log 10\ (N^{-0.108}) \tag{F-2}$$

$$S \ \propto \ N^{-0.108} \tag{F-3}$$

$$S \ \propto \ \left(\frac{1}{N}\right)^{1/9.26} \tag{F-4}$$

$$S^{9.26} \ \propto \ \left(\frac{1}{N}\right) \tag{F-5}$$

$$NS^{9.26} = \text{constant} \tag{F-6}$$

Now consider a reference test using index 1 and an equivalent test using index 2.

$$N_1 S_1^{9.26} = N_2 S_2^{9.26} \tag{F-7}$$

$$\frac{N_2}{N_1} = \left(\frac{S_1}{S_2}\right)^{9.26} \tag{F-8}$$

Assume linear behavior. A doubling of the stress value requires 1/613 times the number of reference cycles. Thus, if the acceleration GRMS level is doubled, then an equivalent test can be performed in 1/613 th of the reference duration, in terms of potential fatigue damage. This is also shown by considering the numerical experiment results of Tables 4 and 5.